Available online at www.sciencedirect.com

SciVerse ScienceDirect

Ceramics International 38 (2012) 4923–4928

CERAMICS INTERNATIONAL

www.elsevier.com/locate/ceramint

Electrical properties and microstructural evolution of ZrO_2–Al_2O_3–TiN nanocomposites prepared by spark plasma sintering

Songlin Ran [a,b], Lian Gao [b,*]

[a] Anhui Key Lab of Metal Materials and Processing, School of Materials Science and Engineering, Anhui University of Technology, Ma'anshan, Anhui 243002, PR China

[b] State Key Lab of High Performance Ceramics and Superfine Microstructure, Shanghai Institute of Ceramics, Chinese Academy of Science, Shanghai 200050, PR China

Received 13 September 2011; received in revised form 23 February 2012; accepted 27 February 2012
Available online 5 March 2012

Abstract

Electroconductive ZrO_2–Al_2O_3–25 vol% TiN ceramic nanocomposites were prepared by spark plasma sintering at 1200 °C for 3 min. The electrical resistivity of the composites decreased from 4.5×10^{-4} Ω m to 3×10^{-5} Ω m as the Al_2O_3 content in the ZrO_2–Al_2O_3 matrix increased from 0 to 100 vol%. SEM images graphically presented the microstructural evolution of the composites and a geometrical percolation model was applied to investigate the relationship between the electrical property and the microstructure. The results indicated that the addition of Al_2O_3 to ZrO_2–TiN improved the electrical conductivity of the material by tailoring the structure from ''nano–nano'' type for ZrO_2–TiN to ''micro–nano'' type for ZrO_2–Al_2O_3–TiN.

Keywords: A. Sintering; C. Electrical conductivity; D. Al_2O_3; D. ZrO_2

1. Introduction

Ceramic composite is one of the most important structural materials due to their outstanding mechanical properties and corrosion resistance [1]. Moreover, some ceramic composites show functional properties, such as electroconductivity, zero temperature coefficient of resistivity (ZTC) and magnetism, machinability [2–5]. These materials can be named as structure and function integrated materials which have potential applications in many fields [2–5].

Recently, electroconductive ceramic composites have been intensively investigated as structure and function integrated materials because these materials not only have excellent mechanical properties but also show high electrical conductivity [2,6–9]. They can replace conventional metal parts in special electronic devices and fabricate complex-shaped ceramic components through electrical discharge machining (EDM). For example, our group reported that incorporating 5–25 vol% TiN particles into the Al_2O_3 matrix could increase the 3-point bending strength of the composite from 370 MPa to 725 MPa while the electrical resistivity of composites could be decreased to less than 10^{-5} Ω m [7]. Liu et al. showed different shapes of Si_3N_4–TiN composites machined by EDM technique, such as vertical walls, micro-hole, micro-gear and micro-gear hole [8,9].

Usually, Al_2O_3 and ZrO_2 are applied as matrixes in fabricating structural ceramic composites. Both of them are oxides and have good oxidation resistance at high temperature. Al_2O_3 is cheap and hard, easy to be sintered but its strength and fracture toughness are low [7]. ZrO_2 has high strength, superexcellent fracture toughness but with low hardness [10]. TiN is an important material with extreme hardness and excellent electrical conductivity [7]. ZrO_2–Al_2O_3–TiN, the composite of the above three materials, may have better performance by inheriting excellent properties from its components. Sun et al. prepared the ZrO_2–Al_2O_3–TiN composites by hot-pressing sintering technique [11]. For the ZrO_2–19 wt% Al_2O_3–5 wt% TiN composite, the flexural strength, fracture toughness and Vickers hardness were about 1.3 GPa, 12 MPa $m^{1/2}$ and 15.2 GPa, respectively [11].

The previous researches on ZrO_2–Al_2O_3–TiN composites mostly focused on the fabrication process and mechanical properties [11–13]. Little attention has been paid to the

* Corresponding author. Tel.: +86 21 52412718; fax: +86 21 52413122.
E-mail address: liangao@mail.sic.ac.cn (L. Gao).

0272-8842/$36.00
doi:10.1016/j.ceramint.2012.02.084

electrical properties. In the present study, the electrical conductivity of ZrO_2–Al_2O_3–25 vol% TiN composites prepared by a novel spark plasma sintering (SPS) technique were assessed. The result indicated that the electrical conductivity of the composites was improved significantly with the increasing Al_2O_3 content. The microstructure of the composite which is closely related to the electrical properties was also investigated.

2. Experimental procedure

Commercial available ZrO_2 (TZ-3Y-E, 27 nm, Tosoh, Tokyo, Japan), Al_2O_3 (400 nm, Wusong Fertilizer Factory of Shanghai, Shanghai, China) and TiN (20 nm, Hefei Kaier Nanometer Technology Development Co. Ltd., Hefei, China) powders were used as starting materials. The starting powders were mixed homogeneously by ball milling in absolute ethanol on a shaker-mixer (Turbula T2C, Bachoffen, Switzerland) for 24 h, using ZrO_2 beads (YTZ, Φ = 5 mm, Tosoh, Tokyo, Japan) as grinding media. After drying, the obtained powders were sieved with a 200-mesh sieve. For sintering, the powders were poured into a graphite die with an inner diameter of 15 mm lined with a graphite paper. The sintering process was conducted by a SPS apparatus (Dr Sinter 2040, Sumitomo Coal Mining Co. Ltd., Kawasaki, Japan) in an N_2 atmosphere. The specimens were heated at 100 °C/min to 1200 °C and hold for 3 min, then the current was shut off and the specimens were cooled to room temperature in about 20 min. The pressure applied was 50 MPa from the start to the end of dwell time. After the hold, the pressure was removed gradually within 5 min.

After grinding to remove the surface impurities, the density of the ceramic was measured by the Archimedes method in distilled water. The phase composition of the bulk ceramics was characterized by X-ray diffraction (XRD, D/MAX-2550 V, Rigaku. Tokyo, Japan). The room temperature electrical resistivity of the ceramic was measured by the 4-probe method, using Keithley 2410 sourcemeter and Keithley 2000 digit-multimeter (Keithley Instruments, Cleveland, OH) to monitor the current and voltage, respectively. Vickers hardness was carried out on a hardness tester (Wilson-Wolpert Tukon 2100B, Instron, Norwood, MA) with a load of 5 kg and a dwelling time of 10 s. Microstructure of the ceramic was examined by a field emission scanning electron microscopy (FESEM, JSM-6700F, JEOL, Tokyo, Japan).

3. Results and discussion

In this study, the TiN content in the ZrO_2–Al_2O_3–TiN composite was confined to 25 vol% while the Al_2O_3 content in the ZrO_2–Al_2O_3 matrix varied from 0 to 100 vol %. Density measurement indicated that the samples sintered at 1200 °C for 3 min had a high densification degree. The relative densities of the SPSed samples were all higher than 98.5% which could be comparable to those hot-pressed grades sintered at 1500–1550 °C for 30–60 min [11,14]. The result implied that the SPS sintering technique could largely decrease the sintering temperatures of the composites. Due to the higher hardness of Al_2O_3 than ZrO_2, the Vickers hardness (H) of the ZrO_2–Al_2O_3–TiN composites showed a linear increase with the increasing Al_2O_3 content (z):

$$H = 15.26 + 5.88z\,(\mathrm{GPa}) \quad (1)$$

Fig. 1 shows the XRD patterns of ZrO_2–Al_2O_3–TiN composites with different Al_2O_3 contents. Except for ZrO_2, Al_2O_3 and TiN, no new phase was indexed, revealing good chemical compatibility among these three phases. Within the limitation of XRD, no m-ZrO_2 phase was detected in all samples, indicating no obvious spontaneous t-ZrO_2 to m-ZrO_2 phase transformation occurred in the composites during cooling process. This observation is different from the conclusion that the codoping of TiN and Al_2O_3 could induce the $t \rightarrow m$ phase transformation by a relief of internal strain in the t-ZrO_2 lattice due to the microcracks caused by the different thermal expansion coefficient between ZrO_2 and Al_2O_3 [11]. Since only a trace of m-ZrO_2 was detected in the reference, the absence of m-ZrO_2 in this study is understandable if considering the difference of raw materials, sintering process and XRD resolutions [11,14]. According to Fig. 1, the intensity of TiN phase is increasing as Al_2O_3 contents increase from 0 to 100 vol%. Though the volume fraction of TiN in the composites is invariable, its mass fraction increases with increasing Al_2O_3 content due to the lower density of Al_2O_3 (3.98 g cm^{-3}) than ZrO_2 (6.05 g cm^{-3}). Because Al_2O_3 has a lower atomic number than ZrO_2, the XRD intensity for Al_2O_3 peaks is much weaker than that for ZrO_2 in all ZrO_2–Al_2O_3–TiN composites (Fig. 1(b)–(e)). For ZrO_2–TiN composite (Fig. 1(a)), there are two peaks for ZrO_2 phase around 35 and 60°, respectively. With increasing Al_2O_3 (decreasing ZrO_2) content, the XRD intensity for ZrO_2 phase decreased gradually and finally the smaller peaks around 35 and 60° disappeared.

The electrical resistivity of ZrO_2–Al_2O_3–25 vol% TiN composites as a function of Al_2O_3 volume content is

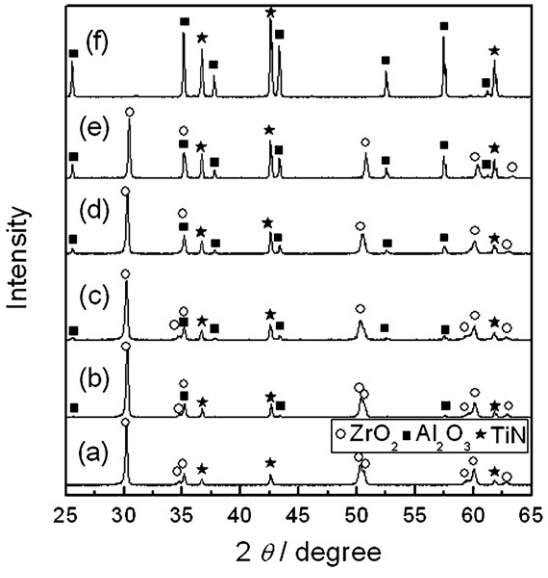

Fig. 1. XRD patterns of ZrO_2–Al_2O_3–25 vol% TiN composites with 0 (a), 20 (b), 40 (c), 60 (d), 80 (e) and 100 vol% (f) Al_2O_3 in the ZrO_2–Al_2O_3 matrix.

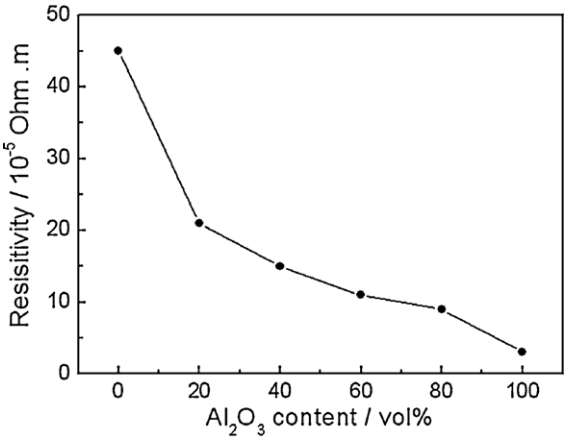

Fig. 2. Electrical resistivity of ZrO_2–Al_2O_3–25 vol% TiN composites as a function of Al_2O_3 volume content in the ZrO_2–Al_2O_3 matrix.

graphically presented in Fig. 2. As the content of Al_2O_3 in the ZrO_2–Al_2O_3 matrix increases from 0 to 100 vol%, the ZrO_2–Al_2O_3–TiN composite exhibits a continuous decrease in resistivity. The electrical resistivity of the Al_2O_3–25 vol% TiN composite is $3.0 \times 10^{-5}\ \Omega$ m, 1 order lower than $4.5 \times 10^{-4}\ \Omega$ m for the ZrO_2–25 vol% TiN composite. According to references, the electrical resistivity of Al_2O_3–20 vol% TiN composites ranged from 10^{-2} to $10^{-5}\ \Omega$ m [7,15,16]. The reported conductive ZrO_2–TiN composites normally had a TiN content over 30 vol% and no report concerned electrical properties of ZrO_2–20 vol% TiN composites [14,17]. For comparison, a ZrO_2–20 vol% TiN composite was prepared by SPS technique. The measured electrical resistivity is over $10^4\ \Omega$ m, at least 6 orders higher than those for Al_2O_3–20 vol% TiN composites. These results indicated that the Al_2O_3–TiN composite possessed higher electrical conductivity than ZrO_2–TiN, especially with low TiN content, despite the fact that Al_2O_3 is more insulating than ZrO_2.

The electrical conductivity of mixtures of conductive and insulating materials is significantly influenced by their microstructures. In general, the conductivity of such mixtures increases drastically as the conductive phase reaches a certain concentration [17]. Different percolation models have been used to understand the conductive behavior of such composites. The model presented by Malliaris and Turner was considered as the most prominent geometrical percolation model [17,18]. In this model, the volume percolation concentration (V_A) symbolizes the onset of conductive network formation and the V_A of a composite is determined by the ratio of diameters of insulating particles (D) and conducting particles (d). The model can be described by the following equation:

$$V_A = 50P_c\left[\frac{1}{1+((\theta/4)(D/d))}\right] \quad (2)$$

where P_c is the first non-zero probability for the occurrence of infinitely long bands of conductive particles on the surfaces of the insulating particles and θ is a quantity to estimate the arrangement of the conductive particles on the surfaces of the insulating ones; the following values are given: hexagonal $P_c = 1/3$, $\theta = 1.11$; cubic $P_c = 1/2$, $\theta = 1.27$; triangular $P_c = 2/3$,

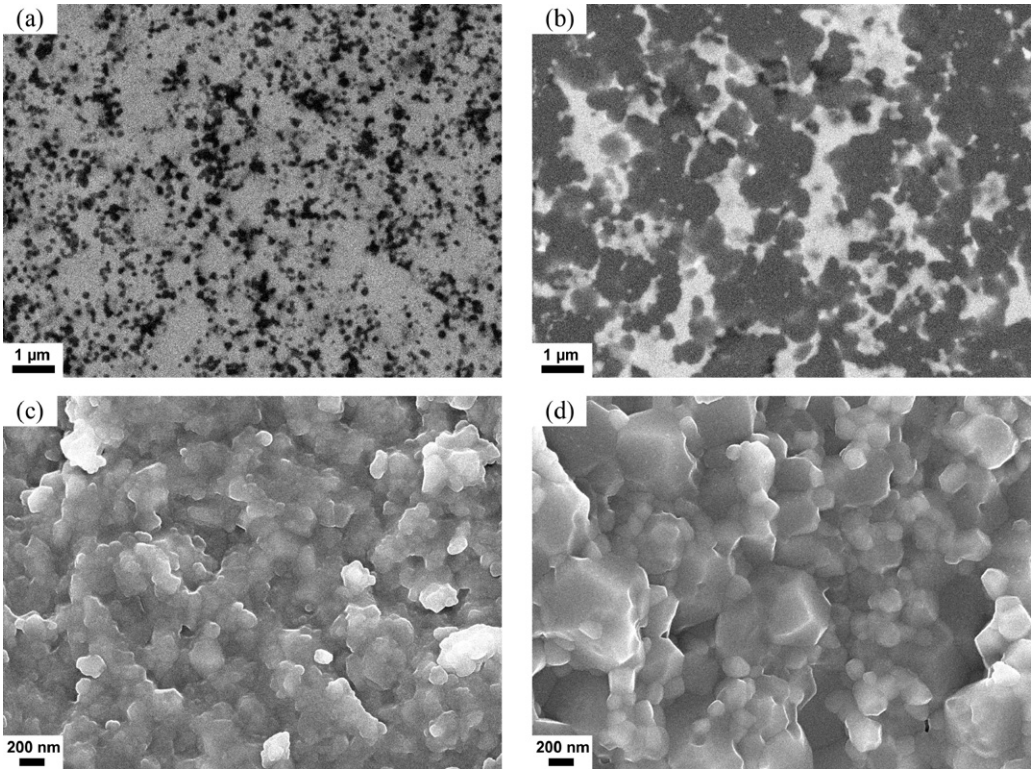

Fig. 3. SEM micrographs of polished (a, b) and fractured (c, d) surfaces of the ZrO_2–25 vol% TiN composite (a, c) and the Al_2O_3–25 vol% TiN composite (b, d). Grain information in (a) white, ZrO_2; dark, TiN; and (b) gray, Al_2O_3; white, TiN.

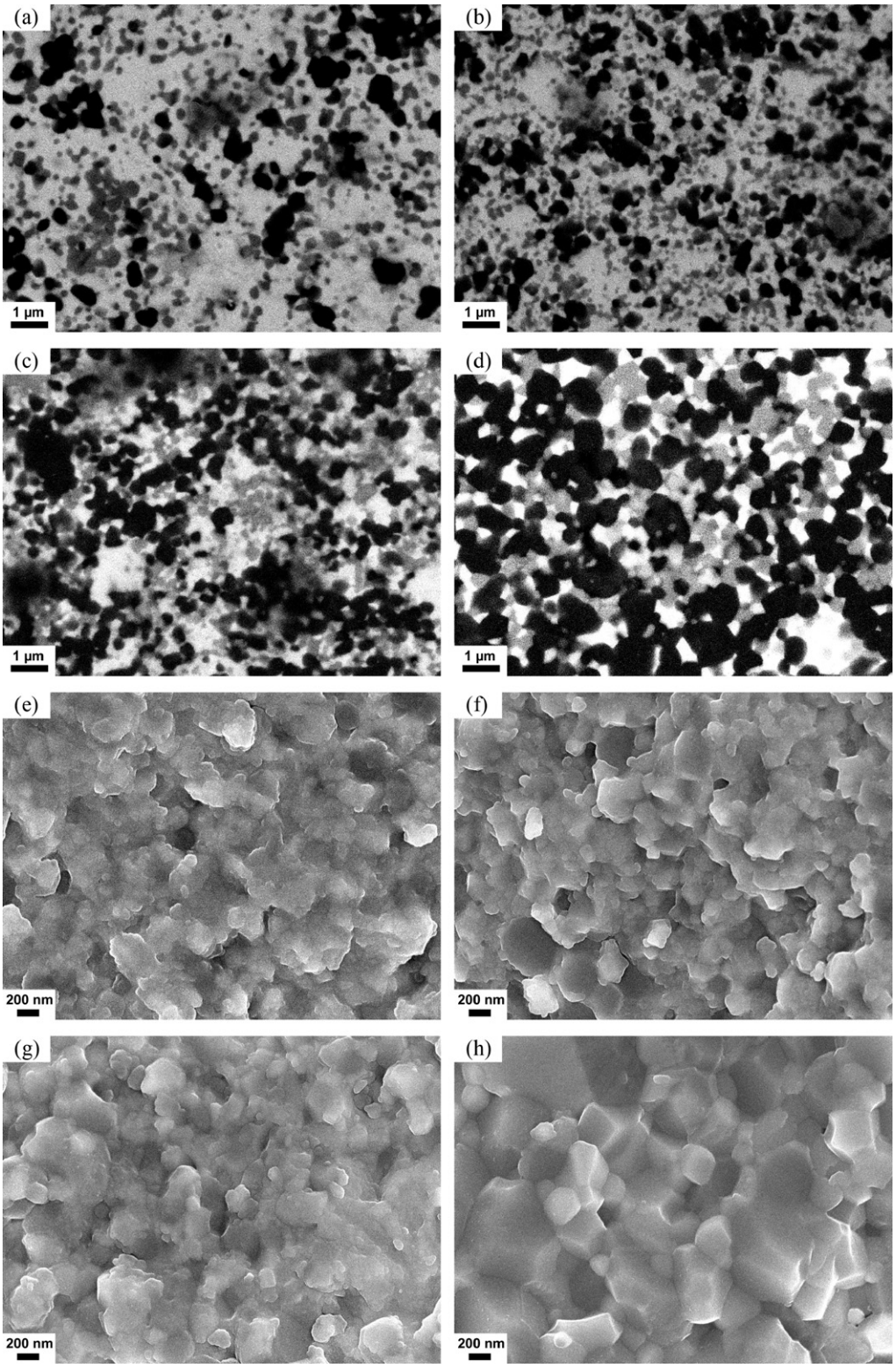

Fig. 4. SEM micrographs of polished (a–d) and fractured (e–h) surfaces of ZrO_2–Al_2O_3–TiN composites with 20 (a, e), 40 (b, f), 60 (c, g) and 80 vol% (d, h) Al_2O_3 in ZrO_2–Al_2O_3. Grain information in (a–d) white, ZrO_2; gray, TiN; dark, Al_2O_3.

$\theta = 1.375$ [6,17,18]. As discussed above, the electrical resistivity of Al_2O_3–20 vol% TiN composites is lower than 10^{-2} Ω m while that for ZrO_2–20 vol% TiN is higher than 10^4 Ω m, suggesting the V_A for Al_2O_3–TiN and ZrO_2–TiN composites is lower and higher than 20, respectively. According to the model, the value of V_A is decided by the values of P_c, θ and D/d which can be assessed according to the microstructures of the composites.

Fig. 3 shows the SEM micrographs of polished and fractured surfaces of ZrO_2–TiN and Al_2O_3–TiN composites with

25 vol% TiN, respectively. In Fig. 3(a), dark TiN grains distribute homogeneously in the white ZrO_2 matrix. TiN powders are nearly monodisperse. There is not much contact between adjacent TiN particles. The conducting network is just beginning to form. In Fig. 3(b), white grains are TiN and gray grains are Al_2O_3 matrix due to the higher atomic number of TiN than Al_2O_3. TiN grains agglomerate together, making them touch with each other and a perfect conducting network is formed. Obviously, it is easier for TiN to form conducting network in Al_2O_3 matrix than in ZrO_2, which agrees with the measured electrical resistivity values.

From Fig. 3(c), it can be seen that all grains in ZrO_2–TiN composite have nearly the same size of around 100 nm and the composite is ''nano–nano'' type nanostructured ceramic. However, there are two different sizes of grains corresponding two phases in Fig. 3(d). The bigger grains are Al_2O_3 and the smaller ones are TiN. TiN grains are nano-sized (around 100 nm) and locating in the boundaries of micro-sized Al_2O_3 grains (about 460 nm). The Al_2O_3–TiN composite is ''micro–nano'' type nanostructured ceramic. The estimated value of D/d is 1.0 for ZrO_2–TiN and 4.6 for Al_2O_3–TiN composite, respectively. If the values of P_c for both materials are set as 0.5 and those of θ are both set as 1.27, the calculated V_A for ZrO_2–TiN is 19, much higher than 10 for Al_2O_3–TiN. The application of the model confirms that the Al_2O_3–TiN composite has lower volume percolation concentration and is easier to form conducting network than ZrO_2–TiN.

According to the above discussion, the electrical resistivity of ceramic composites containing conductive and insulating phases could be controlled by tailoring their microstructures. Normally, in order to save costs, the proportion of conductive phases in the electroconductive ceramics was designed to as less as possible. Enlarging the grain size of matrix could decrease the V_A value and improve the conductivity of the materials. As a result, using less conductive phase could reach the same even higher conducting level. For example, our group reported an Al_2O_3–TiN nanocomposite prepared by a selective matrix grain growth method [19]. With only 12 vol% TiN, the composites showed an unprecedentedly low resistivity of $8 \times 10^{-5}\ \Omega$ m, which was more than two orders lower than the ordinary Al_2O_3–TiN nanocomposite [19].

In this study, it should be noticed that the resistivity curve in Fig. 2 shows a sharp decrease when the matrix of the composite is changed from ZrO_2 to ZrO_2–Al_2O_3. This observation implied the addition of Al_2O_3 could significantly improve the electrical conductivity of the ZrO_2–TiN composite. The incorporating Al_2O_3 particles changed the microstructure of the composite and perfected the conducting network, making the composite more conductive. Fig. 4 presents the microstructural evolution of ZrO_2–Al_2O_3–TiN composites with increasing Al_2O_3 content. Fig. 4(a)–(d) shows the backscattered SEM micrographs of polished surfaces. Three phases, white ZrO_2, black Al_2O_3 and gray TiN, can be distinguished. No pore is found suggests that all composites were fully densified. With the increasing Al_2O_3 content, more and more TiN grains connect with each other and more perfect is the conducting network. According to the SEM micrographs of fracture surfaces of the composites, as illustrated in Fig. 4(e)–(h), the structure of the ZrO_2–Al_2O_3–TiN composite is being changed from ''nano–nano'' to ''micro–nano'' type, which enlarges the value of D/d and results in the decrease of electrical resistivity [6,17,18]. As mentioned earlier, the resistivity of SPSed ZrO_2–20 vol% TiN is higher than $10^4\ \Omega$ m, it can be speculated that adding appropriate amount of Al_2O_3 could improve the conductivity to satisfy the EDM demands.

4. Conclusion

Dense ZrO_2–Al_2O_3–25 vol% TiN nanocomposites were fabricated by spark plasma sintering. The composites showed good sinterability and could be densified at a low temperature of 1200 °C for 3 min. The electrical resistivity of the ZrO_2–Al_2O_3–TiN composite decreased with increasing Al_2O_3 content. SEM analysis and the application of geometrical percolation model indicated that the addition of Al_2O_3 could improve the electrical conductivity of the composite by changing the microstructure from ''nano–nano'' type for ZrO_2–TiN to ''micro–nano'' type for ZrO_2–Al_2O_3–TiN.

Acknowledgment

This work was supported by the Young Teachers' Foundation of Anhui University of Technology (QZ201105).

References

[1] M. Sternitzke, Structural ceramic nanocomposites, J. Eur. Ceram. Soc. 17 (1997) 1061–1082.
[2] C.H. Lee, H.H. Lu, C.A. Wang, P.K. Nayak, J.-L. Huang, Microstructure and mechanical properties of TiN/Si_3N_4 nanocomposites by spark plasma sintering (SPS), J. Alloys Compd. 508 (2010) 540–545.
[3] B. Fu, L. Gao, Tantalum nitride/copper nanocomposite with zero temperature coefficient of resistance, Scripta Mater. 55 (2006) 521–524.
[4] S.T. Oh, M. Sando, K. Niihara, Processing and properties of Ni–Co alloy dispersed Al_2O_3 nanocomposites, Scripta Mater. 39 (1998) 1413–1418.
[5] L. Gao, X.H. Jin, J.G. Li, Y.G. Li, J. Sun, BN/Si_3N_4 nanocomposite with high strength and good machinability, Mater. Sci. Eng. A 415 (2006) 145–148.
[6] Z. Guo, G. Blugan, R. Kirchner, M. Reece, T. Graule, J. Kuebler, Microstructure and electrical properties of Si_3N_4–TiN composites sintered by hot pressing and spark plasma sintering, Ceram. Int. 33 (2007) 1223–1229.
[7] J.G. Li, L. Gao, J.K. Guo, Mechanical properties and electrical conductivity of TiN–Al_2O_3 nanocomposites, J. Eur. Ceram. Soc. 23 (2003) 69–74.
[8] C.C. Liu, Microstructure and tool electrode erosion in EDMed of TiN/Si_3N_4 composites, Mater. Sci. Eng. A 363 (2003) 221–227.
[9] C.C. Liu, J.L. Huang, Effect of the electrical discharge machining on strength and reliability of TiN/Si_3N_4 composites, Ceram. Int. 29 (2003) 679–687.
[10] S.L. Ran, L. Gao, Mechanical properties and microstructure of TiN/TZP nanocomposites, Mater. Sci. Eng. A 447 (2007) 83–86.
[11] J. Sun, C. Huang, J. Wang, H. Liu, Mechanical properties and microstructure of ZrO_2–TiN–Al_2O_3 composite ceramics, Mater. Sci. Eng. A 416 (2006) 104–108.
[12] D. Ostrovoy, N. Orlovskaya, V. Kovylyaev, S. Firstov, Mechanical properties of toughened Al_2O_3–ZrO_2–TiN ceramics, J. Eur. Ceram. Soc. 18 (1998) 381–388.

[13] Y.G. Gogotsi, N.A. Orlovskaya, V.A. Goncharuk, Investigation of the mechanical properties of materials of the system Al_2O_3–ZrO_2–TiN, Powder Metall. Met. Ceram. 32 (1993) 541–543.
[14] S. Salehi, O. van der Biest, J. Vleugels, Electrically conductive ZrO_2–TiN composites, J. Eur. Ceram. Soc. 26 (2006) 3173–3179.
[15] A. Bellosi, G. de Portu, S. Guicciardi, Preparation and properties of electroconductive Al_2O_3-based composites, J. Eur. Ceram. Soc. 10 (1992) 307–315.
[16] Z.S. Rak, J. Czechowski, Manufacture and properties of Al_2O_3–TiN particulate composites, J. Eur. Ceram. Soc. 18 (1998) 373–380.
[17] F. Lux, Models proposed to explain the electrical conductivity of mixtures made of conductive and insulating materials, J. Mater. Sci. 28 (1993) 285–301.
[18] A. Malliaris, D.T. Turner, Influence of particle size on the electrical resistivity of compacted mixtures of polymeric and metallic powders, J. Appl. Phys. 42 (1971) 614–618.
[19] X.H. Jin, L. Gao, Preparation of a highly conductive Al_2O_3/TiN interlayer nanocomposite through selective matrix grain growth, J. Am. Ceram. Soc. 89 (2006) 1129–1132.